Metal Bis(benzylthiolates): Efficient Single Source Precursors to Solid Solutions and Nanoparticles of Metal Sulfides

Philip Boudjouk,*,† Bryan R. Jarabek,† Duane L. Simonson,† Dean J. Seidler,† Dean G. Grier,† Gregory J. McCarthy,† and Lindsay P. Keller‡

Center for Main Group Chemistry, Department of Chemistry, North Dakota State University, Fargo, North Dakota 58105, and MVA, Inc., 5500 Oakbrook Parkway, Suite 200, Norcross, Georgia 30093

Received October 8, 1997. Revised Manuscript Received June 17, 1998

The preparation of solid solutions of the sulfides of zinc, cadmium, and lead has been attempted by low-temperature pyrolysis (150−400 °C) of metal bis(benzylthiolate) precursors. The (Zn,Cd)S shows solid solution behavior at 200−400 °C and crystallite sizes of ∼5 nm. The CdS−PbS system was also prepared by the precursor decomposition method, exhibiting interesting behavior in the lead-rich region. The 150 °C pyrolysis of $Pb(SBn)_2$ leads to nanocrystalline (20−40 nm) PbS single crystals distributed throughout the nanocrystalline (∼2−5 nm) regions of CdS. Pyrolysis at 200 °C produced 40−60 nm PbS cubes dispersed throughout nanocrystalline (∼2−5 nm) CdS. The solids produced were characterized by X-ray powder diffraction, scanning electron microscopy, transmission electron microscopy, selected area electron diffraction, energy-dispersive X-ray analysis, and elemental analysis.

Introduction

The use of single-source precursors for the production of main group and transition metal materials has attracted much interest because of the potential for applications in electronics, optics, and optoelectronics.[1−4] The late transition metal sulfides, with band gaps from the visible to the UV, have important applications as phospholuminescent materials, chemical sensors, radiation (infrared, visible, and ultraviolet) detectors, and compound semiconductor laser materials.[5−11]

Several recent reports[1,12−14] have mentioned the affect of precursor structure and/or decomposition temperature on crystalline phase and offer another means of control not possible with the traditional heating and grinding of the elements. The production of cubic gallium sulfide from the *tert*-butyl derivative of the gallium−sulfur cubane is one of the more striking examples of such control of the crystalline phase. Other examples are the well-known *N*,*N*-dialkyl dithiocarbamates, which have shown utility as single source precursors for the 12−16 and 1−13−16 (formerly group I−III−VI) solar cell materials copper indium selenide and copper gallium sulfide.[15,16]

Recently, the low-temperature pyrolyses of lead and tin bis(butylthiolate) isomers were reported, demonstrating that, for those derivatives, an important driving force for the reaction is the stability of the dissociated fragments, as exemplified by the favored formation of *tert*-butyl radicals.[17,18] However, product analysis revealed substantial contamination by elemental lead and a distribution of volatile byproducts, consistent with the operation of several decomposition mechanisms.

Osakada and Yamamoto[19] reported that metal bis(methylthiolate) derivatives of Zn and Cd produce cubic solid solutions of $(Cd_x,Zn_{1-x})S$ (x = 0.25, 0.52, 0.78) at 260−280 °C. This paper also stated that the phenylthiolate derivatives, studied by Dance et al.,[20] are

† North Dakota State University.
‡ MVA, Inc.

(1) Cowley, A. H.; Jones, R. A. *Polyhedron* **1994**, *13*, 1149.
(2) Brennan, J. G.; Siegrist, T.; Carroll, P. J.; Stuczynski, S. M.; Reynders, P.; Brus, L. E.; Steigerwald, M. L. *Chem. Mater.* **1990**, *2*, 403.
(3) Hirpo, W.; Dhingra, S.; Sutorik, A. C.; Kanatzidis, M. G. *J. Am. Chem. Soc.* **1993**, *115*, 1597.
(4) Steigerwald, M. L.; Sprinkle, C. R. *J. Am. Chem. Soc.* **1987**, *109*, 7200.
(5) Haase, M. A.; Qiu, J.; DePuydt, J. M.; Cheng, H. *Appl. Phys. Lett.* **1991**, *59*, 1272.
(6) Nurmikko A.; Pratt, G., Jr. *Appl. Phys. Lett.* **1975**, *27* (2), 83.
(7) Young J.; Zemel, J. *Appl. Phys. Lett.* **1975**, *27* (8), 456.
(8) Assenov, R.; Moshnikov, V. A.; Yaskov, D. A. *Phys. Stat. Sol.* **1985**, *88*, K27.
(9) Zogg, H.; Maissen, C.; Masek, J.; Blunier, S.; Lambrecht, A.; Tacke, M. *Semicond. Sci. Technol.* **1990**, *5*, S49.
(10) Haase, M. A.; Baude, P. F.; Hagedorn, M. S.; Qui, J.; DePuydt, J. M.; Cheng, H.; Guha, S.; Höfler, G. E.; Wu, B. J. *IEEE Trans. Elec. Dev.* **1993**, *40* (11), 2110.
(11) Jeon, H.; Ding. J.; Patterson, W.; Nurmikko, A. V.; Xie, W. Grillo, D. C.; Kobayashi, M. Gunshor, R. L. *Appl. Phys. Lett.* **1991**, *59* (27), 3619.
(12) Kräuter, G.; Neumueller, B.; Goedken, V.; Rees, W., Jr. *Chem. Mater.* **1996**, *8*, 360.
(13) Cleaver, W. M.; Späth, M.; Hynk, D.; McMurdo, G.; Power, M.; Stuke, M.; Rankin, D. W. H.; Barron, A. F. *Organometallics* **1995**, *14*, 690.
(14) Rees, W. S., Jr.; Kräuter, G. *Mater. Res. Soc. Symp. Proc.* **1994**, *327*, 3.
(15) Hepp, A. F.; Hehemann, D. G.; Duraj, S. A.; Clark, E. B.; Eckles, W. E.; Fanwick, P. E. *Mater. Res. Soc. Symp. Proc.* **1994**, *327*, 29.
(16) Wold, A.; Dwight, K. *Solid State Chemistry* Chapman and Hall: New York, 1985.
(17) Kräuter, G.; Favreau, P.; Rees, W. S., Jr. *Chem. Mater.* **1994**, *6*, 543.
(18) Kräuter, G.; Favreau, P.; Nunnally, B. K.; Rees, W. S., Jr. *Mater. Res. Soc. Symp. Proc.* **1994**, *327*, 41.
(19) Osakada, K.; Yamamoto, T. *J. Chem. Soc., Chem. Commun.* **1987**, 1117.

S0897-4756(97)00669-8 CCC: $15.00
Published on Web 08/29/1998

potential precursors for thin films. The synthesis of cubic (Zn,Cd)S solid solutions was later reported by the vapor phase decomposition of dialkylmetal and methyl mercaptan.[21]

Metal bis(arenethiolates) have also been pyrolyzed,[22] sometimes producing the unexpected high-temperature phase of 12−16 materials,[23] but in most cases, the solid products were not fully investigated and the volatile components of the reaction mixtures contained products resulting from reductive elimination and radical recombination processes. Even the well-characterized crystalline 14−16 precursors reported by Seligson and Arnold,[24] with no carbon attached directly to metal or chalcogen, gave hydrocarbon impurities in the ceramic materials. Only recently have others shown the use of arene chalcogenides with bulky and/or coordinating substituents [25,26] to enhance volatility for vapor deposition studies.

We have been exploring the unexpected utility of phenyl groups as mobile ligands in single-source precursors to low carbon contaminated group 14−16[27,28] and group 13−15[29] materials. The high yield production, on the gram scale, of binary and ternary materials from perphenylated derivatives of elements from these groups is attributed to the facility with which phenyl groups migrate when attached to heavy atoms. Access to a low-energy rearrangement pathway provided a more efficient alternative to homolytic cleavage of phenyl−metal or phenyl−nonmetal bonds. Encouraged by the success of such a nontraditional route to semiconductors, we explored other routes to these materials that do not rely on the more conventionally employed mechanism of β-hydride or radical elimination of the organic fragments.[1,30,31] While this paper was in preparation, other low-energy dual-source syntheses of amorphous and/or nanocrystalline sulfides in nonaqueous solvents near room temperature were reported elsewhere.[32,33]

We could find no reports of the low-temperature, bulk-phase synthesis of solid solutions of (Pb,Cd)S from single-source organometallic precursors in the literature. This report continues our examination of single-source precursors in the production of solid solutions of main group and transition metal sulfides. The goal of the work was to attempt the synthesis of (Zn,Cd)S and metastable (Pb,Cd)S solid solutions from combinations of zinc, cadmium, and lead bis(benzylthiolate) precursors. The isolation of the metastable solid solutions of the rocksalt-type, (Pb,Cd)S, has been reported in several instances both in bulk and thin films, but all cases required the use of high-temperature/high-pressure or vacuum sublimation equipment.[34,35]

Herein we report that metal bis(benzylthiolates), readily prepared from the metal salts and benzyl mercaptan,[36,37] (eq 1) are efficient single-source precursors to nanocrystalline $(Zn_xCd_{1-x})S$ solid solutions. The cubic phase solid solutions of zinc sulfide and cadmium sulfide obey Vegard's law with slight deviation from the theoretical linear relationship. The hexagonal phase, when present, also exhibits solid solution behavior. The PbS−CdS system gives nanocrystalline materials at temperatures of 150−200 °C. Metastable solid solutions of $(Pb_{1-x}Cd_x)S$ are not formed for $x > \sim 0.02$.

$$MX_2 + C_6H_5CH_2SH \rightarrow M(SCH_2C_6H_5)_2 + 2HX \quad (1)$$

$$M = Pb, Cd, Zn$$

$$X = NO_3, O_2CCH_3$$

Experimental Section

General Procedures. Preparations of the metal bis(benzylthiolates) were carried out in a fume hood under a nitrogen atmosphere using Schlenk techniques for all transfers and manipulations. The metal salts and benzyl mercaptan were purchased from Aldrich and used without further purification. These compounds used are toxic and irritants; therefore, caution and protective clothing must be used when handling them. The 95% ethanol and distilled water solvents were degassed with nitrogen for 15 min before use. Dimethyl sulfoxide solvent for solution pyrolysis experiments was dried over $CaSO_4$ overnight and then distilled from fresh $CaSO_4$ and kept under nitrogen before use. Normal dodecane was passed through a 5 cm column of neutral alumina and directly into the reaction flask cooled under a flow of nitrogen. Infrared spectra were recorded on a Mattson-Galaxy 2020 FTIR with pressed KBr pellets and are reported in cm^{-1}. ^1H and ^{13}C NMR were acquired on a JEOL GSX 400 MHz FT-NMR and are reported relative to Me_4Si in parts per million (ppm).

Scanning electron microscopy (SEM) was performed on a JEOL JSM6300V with the Noran Voyager III microanalysis package for qualitative elemental analysis, and samples were plasma treated with Au to reduce surface charging. The X-ray powder diffraction (XRD) patterns were collected on a Philips automated diffractometer operating in 2θ mode using Ni-filtered Cu Ka radiation with NIST 660 lanthanum hexaboride internal standard. Data analysis was accomplished using the JADE software package from MDI, Inc. Thermogravimetric analysis (TGA) data were obtained on a Perkin-Elmer series 7 instrument using a hold temperature of 60 °C and heating rate of 5 °C/min. Melting point determinations were done on a Thomas-Hoover capillary apparatus and are uncorrected. Elemental analysis was performed on a Perkin-Elmer 2200 series II instrument. GC−MS data was collected on a Hewlett-Packard 5992 quadrupole mass spectrometer. Transmission electron microscopy (TEM) analysis was done on a JEOL 2010 microscope equipped with a NORAN thin window energy-dispersive X-ray (EDX) spectrometer. Samples were prepared by grinding in acetone and placing the resulting suspension on a holey carbon thin film supported by a copper TEM grid.

(20) Craig, D.; Dance, I. G.; Garbutt, R. *Angew. Chem., Int. Ed. Engl.* **1986**, *25*, 165.
(21) Fujita, S.; Funato, M.; Hayashi, S.; Fujita, S. *J. Appl. Phys.* **1989**, *28* (6), L898.
(22) Strzelecki, A. R.; Likar, C. L.; Helsel, B. A.; Utz, T.; Lin, M. C.; Bianconi, P. A. *Inorg. Chem*. **1994**, *33*, 5188.
(23) Brennan, J.; Siegrist, T., Carroll, P.; Stuczynski, S.; Brus, L. E., Steigerwald, M. L. *J. Am. Chem. Soc.* **1989**, *111*, 4141.
(24) Seligson, A.; Arnold, J. *J. Am. Chem. Soc.* **1993**, *115*, 8214.
(25) Bonasia, P.; Arnold, J. *J. Organomet. Chem*. **1993**, *449*, 147.
(26) Cheng, Y.; Emge, T. J.; Brennan, *Inorg. Chem*. **1994**, *33*, 3711.
(27) Bahr, S. R.; Boudjouk, P.; McCarthy, G. M. *Chem. Mater.* **1992**, *4*, 383.
(28) Boudjouk, P.; Seidler, D. J.; Bahr, S. R.; McCarthy, G. J. *Chem. Mater*. **1994**, *6*, 2108.
(29) Pan, Y.; Boudjouk, P. *Main Group Chem*. **1995**,*1*, 61.
(30) Zanella, P.; Rosetta, G.; Brianese, N.; Ossola, F.; Porchia, M.; Williams, J. O. *Chem. Mater.* **1991**, *3*, 225.
(31) Osakada, K.; Yamamoto, T. *Inorg. Chem*. **1991**, *30*, 2328.
(32) Henshaw, G.; Parkin, I. P.; Shaw, G. *Chem. Commun*. **1996**, 1095.
(33) Ohtaki, M.; Oda, K.; Eguchi, K.; Arai, H. *Chem. Commun*. **1996**, 1209.
(34) Sood A., K.; Wu, K.; Zemel, J. N. *Thin Solid Films* **1978**, *48*, 73.
(35) Sood A., K.; Wu, K.; Zemel, J. N. *Thin Solid Films* **1978**, *48*, 87.
(36) Peach, M. *J. Inorg. Nucl. Chem*. **1979**, *41*, 1390.
(37) Shaw, R. A.; Woods, M. *J. Chem. Soc. A* **1971**, 1569.

Syntheses. *$Pb(SCH_2C_6H_5)_2$*. $Pb(O_2CCH_3)_2 \cdot 3H_2O$ (3.05 g, 8 mmol) was dissolved in a degassed solution of 80 mL of H_2O and 20 mL of EtOH and heated to 50 °C. Benzyl mercaptan (1.89 mL, 16 mmol) was added dropwise by syringe and stirred at 50 °C for 20 min. The cooled mixture was then vacuum filtered under vacuum and the solid was washed with chilled EtOH, to give 4.2 g of moist solid. Drying overnight in a vacuum desiccator resulted in 3.5 g (96%) of $Pb(SCH_2C_6H_5)_2$: mp 102−108 °C (dec), lit.[39] mp 95−100 °C (dec); IR (cm^{-1}) 3182 (w) 1491 (w) 1458 (w) 1406 (w) 1231 (w) 775 (w) 695 (vs) 469 (w); ^1H NMR (pyridine-d_5) 4.75 (s, CH_2), 7.10−7.36 ppm (m, C_6H_5). ^{13}C NMR (pyridine-d_5) 32.9 (s, CH_2), 126.6, 128.8, 129.2, 145.8 ppm (s, C_6H_5). Anal. Calcd for $C_{14}H_{14}PbS_2$: C, 37.1; H, 3.06. Found: C, 36.7; H, 3.06

$Zn(SCH_2C_6H_5)_2$. $Zn(O_2CCH_3)_2 \cdot 2H_2O$ (2.50 g, 11.4 mmol) was dissolved in a degassed mixture of H_2O and EtOH. Benzyl mercaptan (2.83 g, 22.8 mmol) was added dropwise by syringe, immediately forming a white precipitate. The precipitate was isolated by filtration, washed with chilled ethanol and distilled toluene, and then dried in a vacuum desiccator overnight: yield 2.89 g, 81%; mp 204−208 °C (dec); IR (cm^{-1}) 3026 (w), 1616 (m), 1552 (w), 1238 (w), 698 (m); ^1H NMR (pyridine-d_5) 5.3 (s, CH_2), 7.1−7.6 ppm (m, 5H); ^{13}C NMR (pyridine-d_5) 31.1 (s, CH_2), 125.7, 128.2, 128.9, 146.9 ppm (s, C_6H_5). Anal. Calcd for $C_{14}H_{14}ZnS_2$: C, 53.9; H, 4.50. Found: C, 53.2; H, 4.40.

$Cd(SCH_2C_6H_5)_2$. $Cd(NO_3)_2 \cdot 4H_2O$ (30.0 g, 97 mmol) was dissolved in a degassed mixture of H_2O and EtOH. Benzyl mercaptan (24 g, 194 mmol) was added dropwise by syringe, immediately forming a white precipitate. The precipitate was isolated by filtration, washed with chilled ethanol and distilled toluene, and then dried in a vacuum desiccator overnight: yield 28 g, 81%; mp 199−206 °C (dec); IR (cm^{-1}) 3028 (w), 1618 (m), 696(m), 621 (m); ^1H NMR (pyridine-d_5) 5.3 ppm (2H) 7.0−7.3 ppm (5H); ^{13}C NMR: (pyridine-d_5) 21.1 ppm (CH_2), 124.6, 128.6, 128.9, 138.9 ppm (s, C_6H_5). Anal. Calcd for $C_{14}H_{14}CdS_2$: C, 46.9; H, 3.91. Found: C, 46.9; H, 3.88.

Procedure for Thermolysis. Thermal decompositions of the metal bis(benzylthiolates) were carried out in a programmable 800 W Lindberg Model 55035 tube furnace. The ends of a glass tube were connected to a nitrogen supply via glass tubing through rubber stoppers. Nalgene tubing connected nitrogen to a paraffin oil bubbler at the end of the tube to monitor the gas flow. The glass tube was thoroughly flushed with nitrogen for 15 min prior to loading the sample. Nitrogen flow was reduced to ca. 30 mL/min during the pyrolysis. For the solid solution attempts, the two precursors were weighed, ground together thoroughly with a mortar and pestle, and then transferred into the ceramic combustion boat. After thermolysis, the oven and tube were cooled to room temperature. The boat containing the ceramic residue was removed, and the condensed volatiles were isolated by rinsing the glass tube with dichloromethane. The amount of volatiles was quantified by GC using a calibration solution of similar concentration.

The solvent pyrolysis experiments were conducted by charging 25 mL of DMSO or *n*-dodecane into a 50 mL round-bottomed flask. The precursor powder (typically 400 mg) was added with a powder funnel, and the reflux was controlled with a silicone oil bath at 220 °C and a water condenser. The typical time for solution pyrolysis experiments was 8 h, and the reaction was kept under a blanket of dry nitrogen. The solvent was removed by pipet. The solid was then rinsed with distilled acetone and suspended in dry ethanol for preparing XRD slides.

Results and Discussion

The thermal decompositions of lead, zinc, and cadmium bis(benzylthiolates) follow eq 2 and show close to theoretical mass balances for products A and B.

$$x\mathrm{M}(\mathrm{SCH_2C_6H_5})_2 + (1-x)\mathrm{M'}(\mathrm{SCH_2C_6H_5})_2 \rightarrow \underset{\text{A}}{(\mathrm{M}_x\mathrm{M'}_{1-x})\mathrm{S}} + \underset{\text{B}}{\mathrm{C_6H_5CH_2SCH_2C_6H_5}} \quad (2)$$

$$\mathrm{M = Cd,\ M' = Pb},\ 0 \le x \le 0.02; \quad \mathrm{M' = Zn},\ 0 \le x \le 1$$

Table 1. Product Distribution from the Pyrolysis of $M(SCH_2C_6H_5)_2$

$M(SCH_2C_6H_5)_2$ pyrolyzed[a]	% yield (theoretical yield)		total mass recovery (%)	% C in metal sulfide[d]
	metal sulfide[b]	$C_6H_5CH_2S$-$CH_2C_6H_5$[c]		
$Pb(SCH_2C_6H_5)_2$	54.2 (52.8)	43.6 (47.2)	97.8	0.41
$Cd(SCH_2C_6H_5)_2$	43.2 (40.2)	57.3 (59.8)	100.5	1.0
$Zn(SCH_2C_6H_5)_2$	34.5 (31.3)	60.5 (68.9)	96.4	1.4

[a] 150−200 °C, nitrogen flow at 1 atm. [b] Yields measured prior to rinse with hydrocarbon solvents. After rinsing, yields were typically ±1% of theoretical. [c] Yields determined by GC by comparison with a calibrated solution of dibenzyl sulfide in dichloromethane. [d] Carbon content by combustion analysis obtained immediately after pyrolysis at 200 °C.

Carbon contamination was consistently about 1%. The isolated yields of metal sulfide were typically higher than theoretical, probably from contamination by dibenzyl sulfide, a product that was detected at pyrolysis temperatures above 150 °C. The pyrolysis runs at 150−200 °C were conducted for 12 h to ensure complete decomposition. Several trial runs for time periods up to 96 h at 200 °C show no significant changes in mass recovery, carbon contamination, or solid residue crystallinity, as characterized by XRD. Annealing the CdS−PbS samples at 400 °C for 3 h resulted in the formation of highly crystalline hexagonal cadmium sulfide and lead sulfide, confirming that the cadmium sulfide was indeed present as an XRD-undetectable form at lower pyrolysis temperatures. The data from the 150−200 °C runs are summarized in Table 1.

In work related to the pyrolysis of precursors with nonconventional ligands, we and others have observed that the benzyl group undergoes facile cleavage from both metals and nonmetals.[38−40] In the systems investigated here, however, the dominant pathway has been shown[12,14] to be elimination of dibenzyl sulfide. We observe only small quantities of 1,2 diphenylethane (<5%) in the product mixtures when the pyrolysis is conducted at temperatures above 300 °C. Pyrolysis of pure dibenzyl sulfide confirms that these temperatures generate 1,2-diphenylethane from the dibenzyl sulfide. Similar results were observed by others[17] in the pyrolysis of di-*tert*-butyl sulfide. We attribute the mild reaction conditions, high yields, and low carbon contamination to the ease with which dibenzyl sulfide forms. The low-energy pathway to dibenzyl sulfide is probably the result of the ability of the benzylic carbon to function as an electrophilic center toward the nucleophilic sulfur atom as shown in Figure 1. The benzylic carbon is more susceptible to this polarization than the sulfur-bearing carbon atoms in alklythiolates or arenethiolates.

The ZnS and CdS can be prepared from this precursor method to give nanocrystalline particles of finely dis-

(38) Baxter, D. V.; Chisolm, M. H.; DiStasi, V. F.; Haubrich, S. T. *Chem. Mater.* **1995**, *7*, 84.
(39) Kräuter, G.; Goedken, V.; Neumueller, B.; Rees, W. S., Jr. *Mater. Res. Soc. Symp. Proc.* **1994**, *327*, 35.
(40) Boudjouk, P.; Seidler, D. J.; McCarthy, G. J. *Chem. Mater.* **1996**, *8*, 1189.

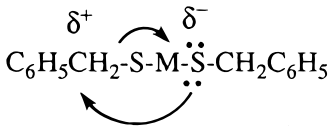

Figure 1. Decomposition mechanism of metal bis(benzylthiolate) precursors.

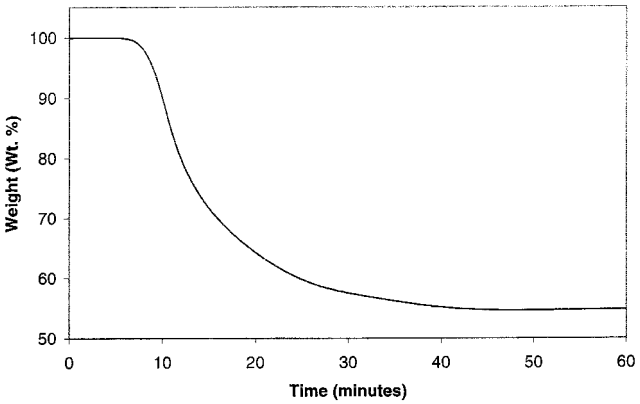

Figure 2. Thermogravimetric analysis of $Pb(SCH_2C_6H_5)_2$ at 150 °C.

persed materials. This work confirms the reports of the thermal decomposition[12,14] of the benzylthiolate group in the formation of group 12 metal sulfides. We also observed the decomposition of lead bis(benzylthiolate) at temperatures as low as 150 °C. We were able to produce nanocrystals of PbS and CdS in the solid state at 150−200 °C or in refluxing solvents such as DMSO or *n*-dodecane.

Thermal Decomposition. The TGA curves of these compounds all show a smooth decomposition at or below 200 °C. The mass decline was used to determine the pyrolysis temperatures for the solid-state decompositions, and the onset temperatures were taken from the software analysis of the mass decline at a threshold of 5%. An isothermal decomposition experiment of $Pb(SCH_2C_6H_5)_2$ at 150 °C gave smooth decomposition to the expected mass, as shown in Figure 2.

Solid-State Characterization. End Member Pyrolysis. X-ray powder diffraction (XRD) was used to check product purity, characterize products by crystal structure, and perform unit cell analysis. The PbS produced at 150, 200, and 400 °C was found to form consistently in the cubic structure (a =5.9362(2) Å), characteristic of galena with a literature value of a = 5.9362 Å, as reported in pattern #5-592 of the Powder Diffraction File (PDF) database. Combustion analyses of the ceramic residues gave values of 4.5% C and 0.51% H at 150 °C and 1.39% C and 0.04% H at 200 °C. These values were reduced at 450 °C to 0.12% C and no detectable amounts of hydrogen. The particles of PbS produced in the solid state were consistently in the 100−300 nm range, as shown in Figure 3.

Zinc sulfide produced at 200−400 °C formed in the cubic sphalerite structure with a = 5.409(3) Å, matching, within experimental error, the literature value of 5.406 reported in pattern #5-566 in the PDF database. Cadmium sulfide was produced at 200 °C in a mixture of the cubic hawleyite and the hexagonal greenockite crystal structures. The Scherrer analysis[41] of these broad peaks gave a crystallite size of ∼5 nm. The inability to isolate either the cubic or hexagonal structures is due to their very similar spatial distributions, causing a lack of important energy differences, as discussed by Wyckoff.[42]

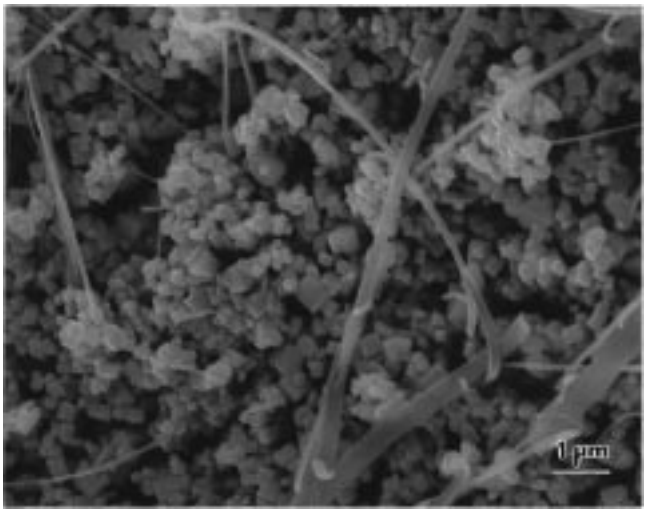

Figure 3. SEM of 100−300 nm PbS particles at 200 °C.

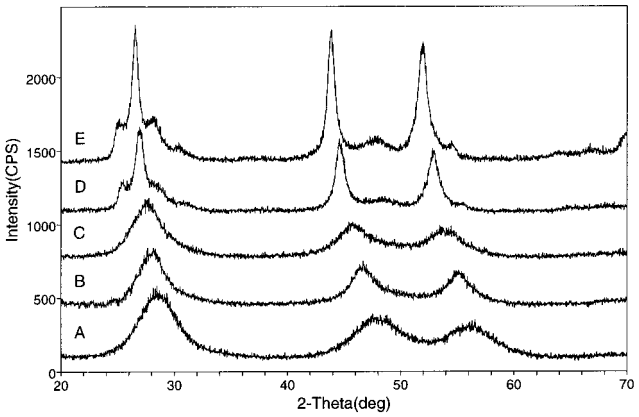

Figure 4. X-ray diffraction patterns of $(Zn_{1-x},Cd_x)S$ from 200 °C pyrolyses. x ranges from 0 in A to 1 in E in 0.25 increments.

Only one major pyrolysis byproduct is seen by GC−MS, suggesting a simple mechanism for decomposition to metal sulfide and dibenzyl sulfide. The volatile material was identified by NMR and GC−MS as dibenzyl sulfide, with only traces of 1,2 diphenylethane. Total mass recovery of the materials was typically 95−100%.

Preparation of Solid Solutions (Zn,Cd)S. The phase diagram of (Zn,Cd)S as solid solution has very little information at temperatures below 400 °C. The addition of CdS to ZnS through the precursor method at 200 °C gives a mixture of the cubic phase and hexagonal phase with an increase in the more favored cubic phase with higher ZnS concentration. At higher CdS concentrations, however, the solid converted to a mixture of the hexagonal (wurtzite) and cubic (sphalerite) phases. The cubic phase was reported[14] for the decomposition of $Cd(SCH_2C_6H_5)_2$ precursor at 250−290 °C.

The XRD patterns from the 200 °C pyrolyses are shown in Figure 4. Patterns A−E show increasing cadmium concentration. Pattern A shows the expected low-temperature form of pure ZnS. When 25 mol % Cd-

(41) Bish, D. L.; Post, J. E. *Modern Powder Diffraction, Reviews in Mineralogy;* Bookcrafters, Inc.: Chelsea, OH, 1989; Vol. 20.
(42) Wyckoff, *Crystal Structures*, 2nd ed.; Krieger: 1986.

Table 2. Unit Cell Analysis of $(Cd_xZn_{1-x})S$ Produced at 200 °C

x	*a* value (Å)	*x*	*a* value (Å)
0.00	5.40	0.75	5.74
0.25	5.52	1.00	5.84
0.50	5.62		

Table 3. Unit Cell Analysis of Cubic $(Cd_xZn_{1-x})S$ Produced at 400 °C

x	*a* value (Å)	*x*	*a* value (Å)
0.00	5.41	0.75	5.73
0.25	5.51	1.00	5.84
0.50	5.61		

$(SCH_2C_6H_5)_2$ is mixed with $Zn(SCH_2C_6H_5)_2$ prior to pyrolysis, the cubic phase still predominates, as in pattern B. The hexagonal phase continues to grow at higher Cd concentrations and becomes a minor phase in C, D, and E. The results of standardless unit cell analysis of the cubic phase at 200 °C are in Table 2. Unit cells were determined by XRD without internal standards due to the nanocrystalline nature of the compounds creating peaks with very large full width at half maximum (fwhm) values. It was therefore not necessary to use standards because the errors corrected by standards are much less than the errors in determining the center of these broad peaks. The unit cell analysis reveals a systematic shift in unit cell dimension, as each increment of 25% Cd shows an increase of about 0.1 Å in the unit cell values of *a*. The unit cell dimension vs composition for the cubic phase agrees with Vegard's law. The hexagonal phase was not present in quantities to allow unit cell analysis for all compositions, but a solid solution behavior could be observed in this phase as well as the cubic phase.

XRD analysis of the solids produced at 400 °C gave similar results (Table 3). The estimation of crystallite size increases to about 12 nm, as expected from the grain growth at higher temperaure. Figure 5 shows the XRD patterns for the various solid solution compositions from 0 to 100% CdS. Significant intensity from the hexagonal phase is present at 50% CdS. The appearance of the hexagonal phase at 400 °C at lower Cd concentrations than at 200 °C agrees with the more stable[43] hexagonal phase of CdS under thermodynamic conditions. A linear relationship of unit cell *a* values with %Cd is observed. The SEM shown in Figure 6 shows the poorly crystalline sample of $(Zn_{0.75},Cd_{0.25})S$ solid solution prepared by this method.

Attempts To Prepare Solid Solutions of (Pb,Cd)S. The goal of this work was the extension of the (Pb,Cd)S solid solution range and the isolation of the cubic [NaCl type] phase of CdS. This phase is normally stable at high pressure, but it has been isolated as a metastable thin film on NaCl substrates and as solid solutions of various metal sulfides. Nanocrystalline particle generation in refluxing solvents was expected to give smaller crystallite size and increase the inherent pressure[44] needed for isolation of the metastable phase in PbS.

Initial examination of diffraction patterns of thermolysis products of intermediate compositions in the

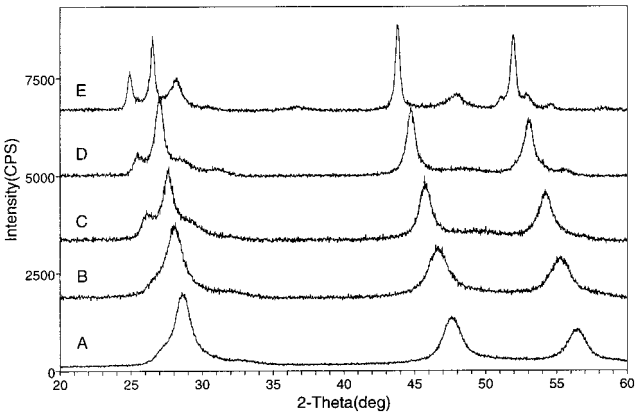

Figure 5. X-ray diffraction patterns of $(Zn_{1-x},Cd_x)S$ from 400 °C pyrolyses with *x* increasing in 0.25 increments from A to E.

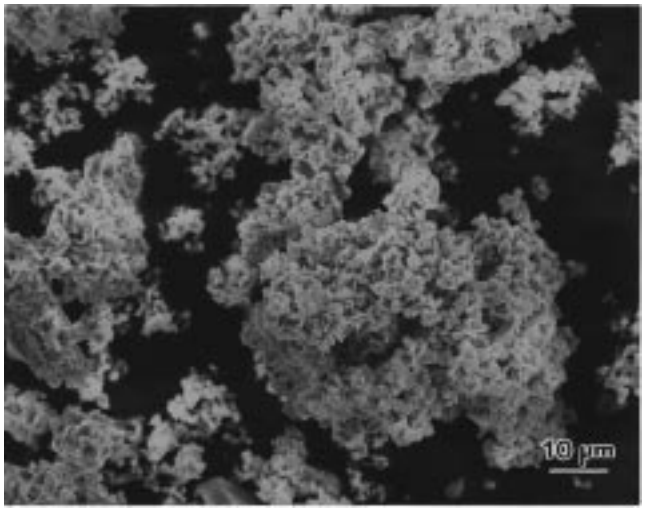

Figure 6. SEM of poorly crystalline $(Zn_{0.75},Cd_{0.25})S$ solid solution.

PbS−CdS system gave the impression that extensive solid solubility of CdS in PbS had occurred. For example, the diffraction patterns appeared to show crystalline phase-pure fcc materials with broad peaks but no peak splitting, which would suggest phase separation, and with no predominant elevations in background scattering, which would suggest one or more amorphous phases. These results seemed to hold true throughout the range of CdS addition until approximately 60% CdS, at which point minor broad hexagonal CdS peaks typical of the end member were observed (Figure 7). However, careful reexamination of background regions containing these peaks in more PbS-rich mixtures revealed barely observable broad hexagonal CdS "peaks" to approximately 30% CdS, but not below.

Despite the implication that solid solutions had formed in samples containing up to 30% CdS, little variation in unit cell parameters was observed across the range of input stoichiometries compared to the end member PbS. Figure 8 shows the calculated shift in unit cell from Vegard's law that was previously confirmed in the metastable synthesis of (Pb,Cd)S epitaxial films.[45] The data shows that very little (∼2%) solid

(43) Huckle, W. G.; Swigert, G. F.; Wiberley, S. E. *Ind. Eng. Chem. Res. Dev.* **1966**, *5* (4), 362.

(44) Haase, M.; Alivisatos, A. P. *J. Phys. Chem.* **1992**, *96*, 6756.

(45) Sood A., K.; Wu, K.; Zemel, J. N. *Thin Solid Films* **1978**, *48*, 73.

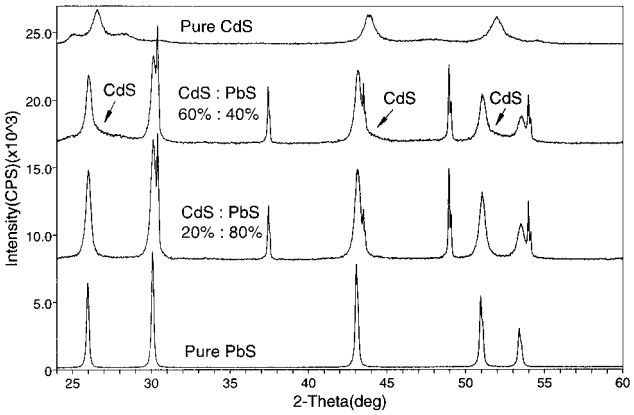

Figure 7. X-ray diffraction patterns of (Pb,Cd)S showing observance of CdS at 60% composition.

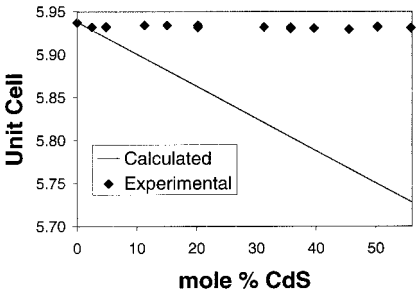

Figure 8. Graph of unit cell vs %Cd of the (Cd,Pb)S system.

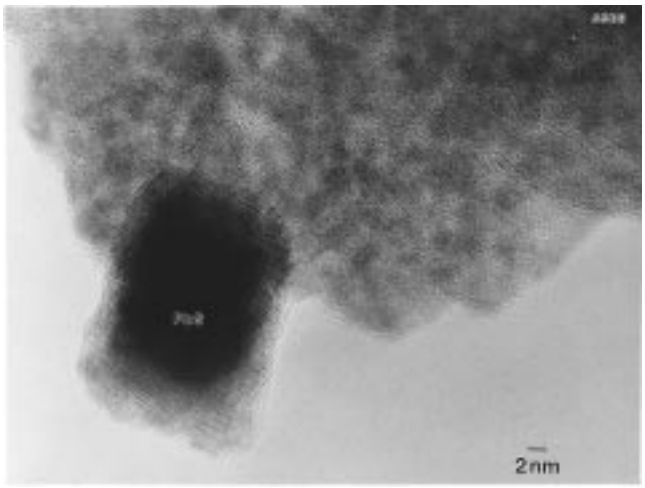

Figure 9. HRTEM of CdS−PbS sample showing a 20 nm rocksalt PbS crystallite intermixed with nanocrystalline (2−5 nm) CdS.

solution had formed at 150 °C, which is consistent with expectations based on the phase diagram.[46] Unfortunately, this interpretation leaves most of the CdS unaccounted for in the system. No cadmium was detected by XRF in the byproducts, which indicated that all of the input cadmium had been retained in the thermolysis product.

TEM analysis was performed to find and characterize the CdS phase. TEM (Figure 9) and SAED showed 20−100 nm crystallites of rocksalt PbS intermixed with nanocrystalline (2−5 nm) CdS. Crystallite sizes of the rocksalt structure phase were consistent with crystallite size estimates obtained from XRD using the Scherrer equation. An important observation for analytical XRD in general was that, although the CdS phase was nearly "X-ray amorphous" in the mixtures, the HRTEM results demonstrated that it is highly crystalline.

EDX analysis of the larger, rocksalt PbS crystallites indicated that no more than 2 mol % Cd could be substituting for Pb in this phase. It is also possible that this small amount of Cd observed by EDX under TEM was present as a thin coating of CdS on larger, pure PbS crystallites. The presence of a small amount of Cd in solid substitution for Pb in the rocksalt structure phase, rather than as a coating, is consistent with the small unit cell shift seen by XRD. For a more detailed discussion of the comparison between TEM and XRD in this study, see the paper by Jarabek et al.[47]

Nanoparticle Generation in Refluxing Solvents. Rees[14] and others[20,23] had previously used the decomposition of precursor molecules in refluxing solvents to generate small particles of semiconductors; thus, the low-temperature decomposition of this precursor system warranted similar experiments. The pyrolysis of lead bis(benzylthiolate) in boiling *n*-dodecane or DMSO gave nanocrystals of lead sulfide, which were confirmed by XRD line broadening estimates of ∼25 nm. SEM analysis showed a broad range of particle sizes, with particle sizes from a fraction of a micrometer up to several microns. Cadmium bis(benzylthiolate) decomposition gave similar XRD effects of peak broadening, and SEM analysis again showed a small particle size.

Pyrolysis of lead and cadmium bis(benzylthiolate) in refluxing solvents near 200 °C resulted in almost no change in the XRD pattern, as compared to the solid-state pyrolysis experiments. The total mass recovery of the metal sulfides and dibenzyl sulfide was not calculated, as some of the nanoparticles produced were suspended in the solvents as colloidal particles.

Conclusions

Complete solid solutions of (Zn,Cd)S are readily prepared at 200 and 400 °C in the solid state by pyrolysis of mixtures of the metal bis(benzylthiolate) precursors. The sphalerite cubic phase dominates in this system, with hexagonal solid solutions also occurring at higher temperatures and higher cadmium concentrations.

Nanocrystalline materials of PbS and CdS and limited solid solutions of (Pb,Cd)S can be readily produced from the solid-state decomposition of the metal bis(benzylthiolate) precursors at temperatures as low as 150 °C. The copyrolysis of cadmium bis(benzylthiolate) and lead bis(benzylthiolate) leads to the formation of consistent sizes of 20−40 nm crystals of lead sulfide in a matrix of 2−5 nm crystals of cadmium sulfide. The solubility of these samples of cadmium sulfide in lead sulfide, approximated from EDX analysis and XRD unit cell analysis, is about 2 wt % cadmium sulfide.

The reported solubility of lead sulfide in hexagonal cadmium sulfide is virtually zero, as the different crystalline phases and large size differences prevent significant substitution in the lattice. The amount of solid solution in this study is significant, as estimated

(46) Leute, V.; Schmidt, R. Z. *Phys. Chem.* **1991**, *172*, 81.

(47) Jarabek, B. R.; Grier, D. G.; Simonson, D. L.; Seidler, D. J.; Boudjouk, P.; McCarthy, G. J. *Adv. X-ray Anal.* **1997**, *40*.

by energy-dispersive X-ray analysis. The comparison with standards reveals up to 2 wt % solubility of lead sulfide in cadmium sulfide, a result certainly not predicted by the phase diagram. The TEM pictures show a possible source of contamination that may affect these solubility estimates, as the outside edges of the PbS crystal studied show regions that may contain amorphous or poorly crystallized CdS material. The exact content of this coating is too small and therefore remains uncertain. The nature of this "coating" of semiconductor may bear resemblance to the study of the coated semiconductor nanoparticles[48] created by injection of lead ions into a solution containing growing nanoparticles of CdS. The lead ions injected into aqueous solutions would tend to displace the cadmium atoms, but not form a true solid solution.

The study of the phase diagram below ~400 °C was not possible with previous synthetic methods, as reaction rates were too slow to allow complete reaction and/or distribution needed for complete randomization of the solid solution components. The solid-state decomposition of metal bis(benzylthiolate) precursors may lead to a novel method for controlling the particle size and distribution of metal sulfides of different crystalline phases or of complete solid solutions.

The ease of synthesis and mild conditions required for thermal decomposition merit the use of benzylthiolate derivatives in semiconductor nanoparticle synthesis. Additional studies may reveal a simple synthetic path to new or metastable phases, possibly with the transition metal sulfides as already shown in the isolation of rocksalt CdS using metal sulfides as additives. The preparation of the benzylthiolate derivatives of zinc, copper, nickel, and other metals may yet prove to be beneficial in isolating metastable or new phases of semiconductor materials.

Acknowledgment. Financial Support from the Office of Naval Research through Grant No. NOO14-96-1-1271 and the National Science Foundation through Grant No. OSR-9452892 is gratefully acknowledged. We thank Dr. Thomas Freeman, Kathy Iverson, and Scott Payne for obtaining the SEM photomicrographs.

CM970669D

(48) Zhou, H. S.; Honma, L.; Komiyama, H.; Haus, J. W. *J. Phys. Chem.* **1993**, *97*, 895.